# Development of non-enzymatic glucose electrode based on Au nanoparticles decorated single-walled carbon nanohorns

**Cheng Bi**
Guangxi Normal University
**Hong-Wei Lv**
Guangxi Normal University
**Hui-Ling Peng** ( penghuiling1008@163.com )
Guangxi Normal University https://orcid.org/0000-0002-2846-2552
**Quan-Fu Li**
Guangxi Normal University

**Original Research**

**Keywords:** Gold nanoparticles, Single-walled carbon nano-horns, Non-enzymatic glucose detection, High sensitivity

**Posted Date:** February 10th, 2021

**DOI:** https://doi.org/10.21203/rs.3.rs-198395/v1



**Version of Record:** A version of this preprint was published at Journal of Materials Science: Materials in Electronics on April 19th, 2021. See the published version at https://doi.org/10.1007/s10854-021-05905-7.

# Abstract

A composite with gold nanoparticles (AuNPs) decorating single-walled carbon nano-horns (SWCNHs) is synthesized and used to modify a gold electrode for non-enzymatic glucose detection. The composite was synthesized by a simple covalent bonding method. The AuNPs with an average particle size of 40 nm are dispersed homogeneously on the surface of the SWCNHs. Therefore, the synergistic effect of the AuNPs and the SWCNHs leads to an excellent glucose sensing performance. The glucose sensing tests indicate that the electrode fabricated has a linear response in the 0.5-2 mM and 4–12 mM glucose concentration range, a high sensitivity (275.33 and 352.5 μA $cm^{-2}$ $mM^{-1}$), and a low detection limit (0.72 μM) (S/N = 3) at + 0.3 V, as well as strong resistance to the interference by ascorbic acid (AA), uric acid (UA), dopamine (DA), galactose, and lactose. When the electrode was used for the detection of glucose in blood samples, the glucose contents detected by the electrode was in right agreement with real. The performance level reached makes the electrode a potential alternative tool for the detection of glucose.


# 1. Introduction

Diabetes mellitus is a metabolic disorder characterized by elevated levels of blood glucose. The number of people with diabetes mellitus is increasing every year. In 2017, the International Diabetes Federation (IDF) estimated that 1 in 11 adults aged 20–79 years (451 million adults) had diabetes mellitus globally and that the number would increase to 693 million in 2045 [1]. According to the IDF, approximately 5 million deaths worldwide were related to diabetes in the 20–99 years age range in 2017, which accounts for 9.9% of the global mortality for people in this age range [2]. Therefore, the detection and monitoring of the glucose levels is essential for the prevention, the diagnosis, and the treatment of diabetes. Many glucose sensors were developed using enzymes to obtain a high sensitivity and good selectivity [3]. However, the sensitivity, the selectivity, and the stability of enzyme-based glucose sensors largely depend on the activity of the enzymes. The pH, the humidity, and the temperature influence the activity of glucose enzymes [4].

To overcome these issues, non-enzymatic glucose sensors have been developed as alternatives [5–8]. Overall, non-enzymatic glucose sensors have many strong advantages, such as a high reproducibility, a high stability, and structural simplicity. To date, many noble metals (Pt, Au, and Pd), transition metals (Cu, Ni, and Co) and their oxides or hydroxides have been used in non-enzymatic glucose sensors [9–15]. Among them, Au is widely used because it produces a high glucose oxidation current in neutral or alkaline conditions [16, 17]. Furthermore, Au nanoparticles (AuNPs) are glucose catalysts that have attracted much attention because of their large surface area, their excellent catalytic activity, and a high resistance to toxic $Cl^-$ [18]. In addition, the favorable structure of the carrier-catalyst composite is a major advantage for sensors [19–21]. The carrier can affect the dispersion of the catalyst, enhance the conductivity and the stability of the material, and make the catalyst work more effectively. Single-walled carbon nano-horns (SWCNHs) are a nanostructured carbon material with horn-shaped sheaths composed of graphene sheets and has a conical structure with a particularly sharp apical angle [22]. Their excellent electrical conductivity, their high specific surface area, and the vast internal space of the SWCNHs make it an

excellent carrier for other particles. Moreover, SWCNHs are produced without using any metal catalyst at a high purity and can be used directly without further purification [23].

Considering the many merits of AuNPs and SWCNHs, we first developed an Au electrode modified with an AuNPs and SWCNHs composite for the detection of glucose. Covalent bonding is used in the preparation of the Au-SWCNHs composite. The method is simple and has a low cost. Additionally, it avoids the use of toxic reagents and the composite performs very well for the electrochemical detection of glucose. SWCNHs have a large surface area and good electrochemical properties [22], which gives the composite prepared a stable structure and a high catalytic activity for glucose. There are enough binding sites for the gold nanoparticles on the modified SWCNHs to enable the formation of s-Au bond. Glucose sensing tests confirmed that the fabricated electrode had high sensitivity, good stability, anti-interference and reproducibility, which is used as the basis for developing the glucose sensor.

## 2. Materials And Methods

# 2.1 Chemicals and apparatus

The SWCNHs were purchased from XFNANO Materials Tech Co., Ltd. Nitric acid ($HNO_3$), sulfuric acid ($H_2SO_4$), cysteamine hydrochloride ($C_2H_7NS{\cdot}HCl$), chloroauric acid ($HAuCl_4$), sodium citrate ($Na_3C_6H_5O_7$), sodium hydrate (NaOH), uric acid (UA), dopamine (DA), ascorbic acid (AA), d-(+)-galactose, lactose, sucrose, and DL-lactic acid were purchased from Sigma-Aldrich. All the chemicals used in this work were of analytical grade and used without further purification.

Scanning electron microscopy (SEM) images were recorded on a JSM-IT300 (JEOL, Ltd., Japan). We used a Renishaw InVia confocal Raman system (Talos F200S, Thermo Fisher Scientific, United States) to examine the defects in the samples. All the electrochemical experiments were performed on a CS2350 electrochemical workstation (Corrtest Instruments Corp., Ltd., Wuhan, China).

# 2.2 Preparation of the Au-SWCNHs composite

The composite comprised of AuNPs decorating SWCNHs was synthesized by a three-step method. First, oxidized SWCNHs (oxSWCNHs) were prepared via a modified Hummers method [24]. We initially mixed 5 ml $H_2SO_4$ (98%) and 15 ml $HNO_3$ (62%). Next, 30 mg SWCNHs were treated with the mixed acid for 16 h under continuous stirring at 50℃ through a hydrothermal reaction. The oxSWCNHs were collected by centrifugation at 12000 rpm for 5 min. Then, the supernatant was removed, and deionized water was added to disperse the oxSWCNHs for further centrifugation. We carried out several rounds of centrifugation and dispersion until the supernatant was neutral. Finally, the oxSWCNHs collected were dried in an oven at 90 ℃. Then, the oxSWCNHs were dispersed into 30 ml of deionized water, and 50 mg of $C_2H_7NS{\cdot}HCl$ were added to the dispersion. The mixture was treated at 90℃ for 24 h with continuous agitation. The mixture obtained was centrifuged at 12000 rpm and washed with deionized water several times. After centrifugation, the composites were placed into deionized water to form a suspended solution, and 5 ml of an $HAuCl_4$ solution (0.01 M) were added. The mixture was sonicated for 30 min to

promote the interaction between the gold ions and the sulfhydryl (-SH) groups of the oxSWCNHs. The mixture was heated to 90 ℃ and 10 ml of a 4% $Na_3C_6H_5O_7$ solution were added. The mixed solution was stirred for 30 min until $Au^+$ was reduced to Au nanoparticles. The dispersion obtained was then centrifuged, washed several times with deionized water, and dried at 90 ℃. The nanocomposite obtained was named Au-SWCNHs. Finally, the Au-SWCNHs black powder was collected and stored at 4 ℃ for further use.

## 2.3 Preparation of the Au-SWCNHs modified Au electrode

Before its modification, the Au electrode was polished, washed several times with deionized water and anhydrous ethanol under sonication, and dried in a nitrogen stream. First, we added 10 mg of the Au-SWCNHs powder prepared into 5 ml of anhydrous ethanol and sonicated the mixture for 20 min to obtain an Au-SWCNHs ethanol suspension at 2 mg $ml^{-1}$. Then, we dropped 5 µL of the Au-SWCNHs ethanol suspension on the Au electrode and let it dry naturally to obtain the Au-SWCNHs/Au electrode (Au-SWCNHs/Au). The electrode was stored at 4 ℃ for further use.

# 3. Results And Discussion

## 3.1. Preparation and characterization of the Au-SWCNHs composites

Figure 1 illustrates the preparation of the Au-SWCNHs composite. First, the SWCNHs were treated with mixed acid ($H_2SO_4/HNO_3$). Upon oxidation, oxygen-containing groups like carboxyl groups (-COOH) were generated on the surface of the SWCNHs. Subsequently, the $C_2H_7NS{\cdot}HCl$ added was ionized in water to produce positively charged sulfur-containing ions while the oxygen-containing groups on the surface of the oxSWCNHs ionized were deprotonated and became negatively charged. Both positively and negatively charged ions were then combined by electrostatic forces. After the addition of $HAuCl_4$, it was dispersed by sonication and fully mixed with the SWCNHs, $H^+$ of -SH was replaced by $Au^{3+}$. Finally, AuNPs were formed when $Au^{3+}$ was reduced by $Na_3C_6H_5O_7$. Fig. S1 in the Supplementary information shows the Raman spectra of the SWCNHs and oxSWCNHs samples. The D band (1334 $cm^{-1}$) and the G band (1564 $cm^{-1}$) of both samples were detected. The intensity ratio of D and G peaks ($I_D/I_G$) is an indicator of the level of defects [25]. The oxSWCNHs (1.24) have a higher $I_D/I_G$ ratio than the original SWCNH (0.53). This indicates the structural deformation of the functional SWCNHs by combing functional groups. The unmodified surface of the SWCNH is inert and does not promote the chemical synthesis of surface materials. Therefore, a surface modification is required to introduce functional groups to provide a large number of chemically active binding sites for the modification by other materials. The functional groups on the surface of the SWCNHs provided binding sites for $C_2H_7NS{\cdot}HCl$ and enabled the further modification with the AuNPs.

Figure 2 shows the SEM images of the SWCNHs and Au-SWCNHs samples. Figure 2a and 2b compares the Au nanoparticles dispersed on the surface of the SWCNHs. Figure 2c shows that several isolated Au nanoparticles were scattered on the SWCNHs surface and most Au nanoparticles were spaced by 40–60 nm, indicating that the Au nanoparticles are well distributed on the SWCNH surface. These spherical Au nanoparticles have a considerably large surface area. They are tightly bound to the surface of the SWCNHs and are evenly dispersed. This structure provides a large number of AuNPs as the electrocatalyst.

Figure 3a and 3b respectively show the elemental composition of oxSWCNHs and Au-SWCNHs determined by energy dispersive spectroscopy (EDS). The modification of the Au nanoparticles clearly leads to the reduction of the oxygen atoms, which is consistent with other results in the literature [26]. When comparing the different samples, the N content was higher in the samples with a higher Au content. This is because the AuNPs modification occurs spontaneously with the formation of an Au-S bond, which binds to the oxSWCNHs via the N-containing $C_2H_7NS{\cdot}HCl$. The AuNPs were successfully synthesized by chemical bonding to the SWCNHs and are expected to have good surface properties in electrochemical sensors.

## 3.2. Electrochemical characterization of the Au-SWCNHs/Au eletrode

A three-electrode cell was used for the electrochemical measurements. It contained a platinum counter electrode, an Ag/AgCl reference electrode, and the modified electrodes as the working electrode. The electrochemical behavior of the Au-SWCNHs/Au electrode and the bare Au electrode was first studied by cyclic voltammetry (CV). Figure 4a shows the cyclic voltammograms obtained for the Au-SWCNHs/Au electrode and the Au electrode in a 1.0 M $H_2SO_4$ solution. A wide anodic peak appeared at 1.1 V for the Au-SWCNHs /Au electrode. It corresponds to the formation of gold oxide ($Au_2O_3$). Additionally, a cathodic peak was observed at 0.87 V due to the reduction of the gold oxide. The blue line in Fig. 5a shows that both redox peaks had the same direction as the red line. The value of the peak current of the Au-SWCNHs/Au electrode was significantly larger than that for the bare Au electrode, which indicated that the surface area of the Au-SWCNHs/Au electrode was larger than that of the bare Au electrode. The larger surface area is due to the unique dispersion of AuNPs on the SWCNHs surface that provides more reactive sites for the redox reaction and the electrocatalytic activity.

Then, we compared the electrochemical glucose sensing with the Au-SWCNHs/Au electrode to that of the bare Au electrode by cyclic voltammetry in a 0.1 M NaOH solution without and with glucose at a scan rate of 20 mV $s^{-1}$. Figure 3b shows the CV response of the Au-SWCNHs/Au electrode. In the absence of glucose (black curve), we observed an anodic oxidation peak from the oxidization of Au to $Au_2O_3$ and a cathodic peak from the reduction of $Au_2O_3$ [27] on the Au-SWCNHs/Au electrode. After the addition of the glucose, the CV of Au-SWCNHs/Au electrode was significantly altered and a series of complex electrochemical processes took place. During the forward scanning, two new oxidation peaks were observed at -0.3 V (peak 1) and at + 0.52 V (peak 2). Peak 1corresponds to the direct electrochemical

oxidation of glucose to gluconolactone. Then, gluconolactone was further oxidized to produce peak 2. The AuOH site is considered as the active site for glucose oxidation and the oxidation of glucose on Au depends largely on the number of AuOH sites available [28]. Usually, the $OH^-$ ions in the NaOH solution adsorb onto the surface of the gold at a certain potential to form an active site. At the low potential of peak 1, the amount of AuOH is very limited and the oxidation of glucose is incomplete. When the potential increases, the amount of AuOH increases and gluconolactone is further oxidized (peak 2). An excessively high potential ( > + 0.52 V) leads to the formation of $Au_2O_3$ and the reduction of the AuOH active site, which terminates the oxidation of gluconolactone. In the reverse scanning, $Au_2O_3$ is reduced and AuOH is regenerated to promote glucose oxidation and a significant anodic peak (peak 3) appears at + 0.2 V. All the peak currents increase with the increasing of concentrations of the glucose, which indicated the Au-SWCNHs/Au electrode is sensitive to the glucose. Figure 3c shows the CV response of the bare Au electrode. Though the curves of the bare electrode are similar with those of Au-SWCNHs/Au electrode, the peak currents of the bare electrode are lower than those of Au-SWCNHs/Au electrode. It indicates that the modification of the Au-SWCNHs composite material significantly improves its catalytic activity for the oxidation of glucose.

Figure 4d shows the CV response of the bare Au electrode and the Au-SWCNHs/Au electrode in a 0.1 M NaOH solution with 8 mM glucose. The current at the Au-SWCNHs/Au electrode was generally higher and a significant peak at + 0.52 V appeared. This indicated that the Au-SWCNHs significantly improved the sensitivity to glucose and further improved the electrochemical performance of the non-enzymatic glucose sensing approach used. Overall, the synergistic effect of the AuNPs and the SWCNHs improves the performance of the detection of glucose.

To determine the voltage at which the continuous injection of glucose must be conducted, the amperometric reaction of the Au-SWCNHs/Au electrode to the addition of 4 mM glucose at different voltages was studied in a 0.1 M NaOH solution (Fig. S2). The electrode had the maximum response at + 0.3 V, which was therefore selected for the subsequent experiments.

To determine the dependence of the electrochemical signals on the glucose concentration, the amperometric reaction of the Au-SWCNH/Au electrode to the continuous injection of glucose was studied at a potential of + 0.3 V in 0.1 M NaOH. Figure 5a shows the corresponding current-time (i-t) curve. The intensity of the current at the electrode increased with the addition of glucose. Figure 5b shows the calibration curve, and both linear ranges with slopes of 413 μA $mM^{-1}$ $cm^{-2}$ and 528.75 μA $mM^{-1}$ $cm^{-2}$, respectively. The sensitivity in the first and second linear range was 275.33 μA $mM^{-1}$ $cm^{-2}$ and 352.5 μA $mM^{-1}$ $cm^{-2}$, respectively. The limit of detection (LOD) was determined experimentally at 0.72 μM with a signal-to-noise ratio (S/N) of 3. Table 1 compares the electrochemical performances of the Au-SWCNHs/Au electrode with other non-enzymatic glucose sensors using AuNPs. The developed electrode had a wider linear concentration range and a higher sensitivity than those of in most of cited reports. The unique structure of Au-SWCNHs creating a large surface area and abundant active sites makes glucose easily migrate to the electrode surface for a high sensitivity.

## 3.3. Selectivity, stability, and reproducibility of the Au-SWCNHs/Au electrodes

To evaluate the selectivity of the Au-SWCNHs/Au electrode, we examined the effects of interfering substances like ascorbic acid (AA), uric acid (UA), dopamine (DA), galactose, lactose, sucrose, which typically coexist with glucose in human serum [29]. Therefore, we tested the Au-SWCNHs/Au electrode in a solution where the molar ratio of glucose to each interfering substance was 10:1. Figure 6 shows that the change in the current was insignificant in the presence of interfering substances while the current was significant with the increment of the glucose. This indicated that Au-SWCNHs/Au electrode has excellent selectivity towards glucose. For the stability study, we determined that the current response remained at 90.4% and 78.3% of the maximum value for 600 s and 2000 s, respectively (Fig. S3). The Au-SWCNHs/Au electrodes were stored in an airtight container at room temperature for 19 days and the current response to 4 mM glucose was checked every other day (Fig. S4). After 15 days of storage, the current response only decreased by 8.6%. To study the influence of environmental variables such as humidity, the fabricated electrode was exposed to air for 3 days and tested under similar conditions. The current response remained around 89%. To evaluate the reproducibility, we prepared five electrodes by the same method and used them to detect 4 mM glucose. The relative standard deviation (RSDs) of the glucose response was less than 8.7%. Overall, our results demonstrated that the Au-SWCNHs/Au electrode had an excellent selectivity towards glucose, a good long-term stability, and good reproducibility.

## 3.4. Real sample analysis

The feasibility of the Au-SWCNHs/Au electrode in the practical application was performed by testing the glucose in human blood serum. The tests were conducted in 0.1 M NaOH solution with 100 μL serum added and the sensing results are shown in Table 2. Glucose was added to human serum with and without glucose continuously, and the detection recovery was 93.50-97.67%. This indicated that Au-SWCNHs/Au electrode here reported can be potentially utilized for the real sample analysis.

## 4. Conclusion

AuNPs with an average particle size of 40 nm were synthesized on SWCNHs using an effective method to produce a stable chemical bond. The nanocomposite-modified electrode had a high sensitivity, a wide linear response, good selectivity, a high stability, and a high reproducibility. The AuNPs and the unique structure of the SWCNHs significantly enhanced the catalytic activity of the electrode for glucose. The stable chemical bond between them greatly improved the performance and the storage of the glucose electrode. The large surface area of the microstructure of the SWCNHs provides a good basis to bind a large number of AuNPs, thereby effectively preventing aggregation and deactivation. Moreover, the excellent conductivity of the SWCNHs results in a faster electron transfer between the Au-SWCNHs composite and the Au electrode. Meanwhile, due to the significant catalytic activity of the Au-SWCNHs/Au electrode in the low concentration range of glucose, the electrode has great potential for the detection of glucose in sweat. We believe that our work opens a new route for the preparation of Au-

SWCNHs composites and sets an example for the production of high-quality nanomaterials for sensing applications.

## Declarations

# Acknowledgements

The authors thank to partly financial support from the National Natural Science Foundation of China (No. 61704035), Natural Science Foundation of Guangxi Province (2017GXNSFBA198125), Guangxi technology projects (AD19110076, AD19110063).

## References

1. Zheng, S.H. Ley, F.B. Hu, Global aetiology and epidemiology of type 2 diabetes mellitus and its complications, Nat. Rev. Endocrinol. 14 (2018) 88–98. https://doi.org/10.1038/nrendo.2017.151.
2. H. Cho, J.E. Shaw, S. Karuranga, Y. Huang, J.D. da Rocha Fernandes, A.W. Ohlrogge, B. Malanda, IDF Diabetes Atlas: Global estimates of diabetes prevalence for 2017 and projections for 2045, Diabetes Res. Clin. Pract. 138 (2018) 271–281. https://doi.org/10.1016/j.diabres.2018.02.023.
3. Niu, X. Li, J. Pan, Y. He, F. Qiu, Y. Yan, Recent advances in non-enzymatic electrochemical glucose sensors based on non-precious transition metal materials: Opportunities and challenges, RSC Adv. 6 (2016) 84893–84905. https://doi.org/10.1039/c6ra12506a .
4. Viswanathan, J. Park, D.K. Kang, J.D. Hong, Polydopamine-wrapped Cu/Cu(II) nano-heterostructures: An efficient electrocatalyst for non-enzymatic glucose detection, Colloids Surfaces A Physicochem. Eng. Asp. 580 (2019). https://doi.org/10.1016/j.colsurfa.2019.123689 .
5. Baghayeri, A. Amiri, S. Farhadi, Development of non-enzymatic glucose sensor based on efficient loading Ag nanoparticles on functionalized carbon nanotubes, Elsevier B.V., 2016. https://doi.org/10.1016/j.snb.2015.11.003 .
6. Tang, Q. Liu, Z. Jiang, X. Yang, M. Wei, M. Zhang, Nonenzymatic glucose sensor based on icosahedron AuPd@CuO core shell nanoparticles and MWCNT, Sensors Actuators, B Chem. 251 (2017) 1096–1103. https://doi.org/10.1016/j.snb.2017.05.090 .
7. Yang, G. Li, G. Wang, J. Zhao, X. Gao, L. Qu, Synthesis of $Mn_3O_4$ nanoparticles/nitrogen-doped graphene hybrid composite for nonenzymatic glucose sensor, Sensors Actuators, B Chem. 221 (2015) 172–178. https://doi.org/10.1016/j.snb.2015.06.110 .
8. Li, C.Y. Guo, C.L. Xu, A highly sensitive non-enzymatic glucose sensor based on bimetallic Cu-Ag superstructures, Biosens. Bioelectron. 63 (2015) 339–346. https://doi.org/10.1016/j.bios.2014.07.061 .
9. Y. Lin, B.B. Karakocak, S. Kavadiya, T. Soundappan, P. Biswas, A highly sensitive non-enzymatic glucose sensor based on Cu/$Cu_2O$/CuO ternary composite hollow spheres prepared in a furnace

aerosol reactor, Sensors Actuators, B Chem. 259 (2018) 745–752. https://doi.org/10.1016/j.snb.2017.12.035 .

10. Wang, X. Yang, C. Hou, M. Zhao, Z. Li, Q. Meng, C. Liang, Fabrication of $MnO_x$ /$Ni(OH)_2$ electro-deposited sulfonated polyimides/graphene nano-sheets membrane and used for electrochemical sensing of glucose, J. Electroanal. Chem. 837 (2019) 95–102. https://doi.org/10.1016/j.jelechem.2019.02.016 .
11. Duan, K. Liu, Y. Xu, M. Yuan, T. Gao, J. Wang, Nonenzymatic electrochemical glucose biosensor constructed by $NiCo_2O_4$@Ppy nanowires on nickel foam substrate, Sensors Actuators, B Chem. 292 (2019) 121–128. https://doi.org/10.1016/j.snb.2019.04.107 .
12. Shu, L. Cao, G. Chang, H. He, Y. Zhang, Y. He, Direct electrodeposition of gold nanostructures onto glassy carbon electrodes for non-enzymatic detection of glucose, Electrochim. Acta. 132 (2014) 524–532. https://doi.org/10.1016/j.electacta.2014.04.031 .
13. Meng, Y. Wen, L. Dai, Z. He, L. Wang, A novel electrochemical sensor for glucose detection based on Ag@ZIF-67 nanocomposite, Sensors Actuators, B Chem. 260 (2018) 852–860. https://doi.org/10.1016/j.snb.2018.01.109 .
14. J. Lee, H.S. Yoon, X. Xuan, J.Y. Park, S.J. Paik, M.G. Allen, A patch type non-enzymatic biosensor based on 3D SUS micro-needle electrode array for minimally invasive continuous glucose monitoring, Sensors Actuators, B Chem. 222 (2016) 1144–1151. https://doi.org/10.1016/j.snb.2015.08.013 .
15. S. Nugraha, C. Li, J. Bo, M. Iqbal, S.M. Alshehri, T. Ahamad, V. Malgras, Y. Yamauchi, T. Asahi, Block-Copolymer-Assisted Electrochemical Synthesis of Mesoporous Gold Electrodes: Towards a Non-Enzymatic Glucose Sensor, ChemElectroChem. 4 (2017) 2571–2576. https://doi.org/10.1002/celc.201700548 .
16. B. Vassilyev, O.A. Khazova, N.N. Nikolaeva, Kinetics and mechanism of glucose electrooxidation on different electrode-catalysts: Part II. Effect of the nature of the electrode and the electrooxidation mechanism, Journal of electroanalytical chemistry and interfacial electrochemistry. 196.1 (1985): 127-144. https://doi.org/10.1016/0022-0728(85)85085-3.
17. Biella, L. Prati, M. Rossi, Selective oxidation of D-glucose on gold catalyst, J. Catal. 206 (2002) 242–247. https://doi.org/10.1006/jcat.2001.3497 .
18. Jeong, J. Kim, Fabrication of nanoporous Au films with ultra-high surface area for sensitive electrochemical detection of glucose in the presence of $Cl^-$, Appl. Surf. Sci. 297 (2014) 84–88. https://doi.org/10.1016/j.apsusc.2014.01.082 .
19. S. Ismail, Q.H. Le, H. Yoshikawa, M. Saito, E. Tamiya, Development of non-enzymatic electrochemical glucose sensor based on graphene oxide nanoribbon - Gold nanoparticle hybrid, Electrochim. Acta. 146 (2014) 98–105. https://doi.org/10.1016/j.electacta.2014.08.123 .
20. A. Shabbir, S. Tariq, M. Gul Bahar Ashiq, W.A. Khan, Non-enzymatic glucose sensor with electrodeposited silver/carbon nanotubes composite electrode, Biosci. Rep. 39 (2019). https://doi.org/10.1042/BSR20181983 .

21. Jeong, D.M. Nguyen, M.S. Lee, H.G. Kim, S.C. Ko, L.K. Kwac, N-doped graphene-carbon nanotube hybrid networks attaching with gold nanoparticles for glucose non-enzymatic sensor, Mater. Sci. Eng. C. 90 (2018) 38–45. https://doi.org/10.1016/j.msec.2018.04.039 .
22. Zhu, G. Xu, Single-walled carbon nanohorns and their applications, Nanoscale. 2 (2010) 2538–2549. https://doi.org/10.1039/c0nr00387e.
23. Zhu, S., Zhao, X. E., You, J., Xu, G., & Wang, H., Carboxylic-group-functionalized single-walled carbon nanohorns as peroxidase mimetics and their application to glucose detection. Analyst, 140(2015), 6398-6403. https://doi.org/10.1039/C5AN01104C .
24. Kumar, R., Naqvi, S., Gupta, N., Gaurav, K., Khan, S., Kumar, P., ... & Chand, S., Bulk synthesis of highly conducting graphene oxide with long range ordering. Rsc Advances, 45(2015), 35893-35898. https://doi.org/10.1039/C5RA01943E.
25. Han, S. Zhang, L. Han, D.P. Yang, C. Hou, A. Liu, Porous gold cluster film prepared from Au@BSA microspheres for electrochemical nonenzymatic glucose sensor, Electrochim. Acta. 138 (2014) 109–114. https://doi.org/10.1016/j.electacta.2014.06.095.
26. Duc Chinh, G. Speranza, C. Migliaresi, N. Van Chuc, V. Minh Tan, N.T. Phuong, Synthesis of Gold Nanoparticles Decorated with Multiwalled Carbon Nanotubes (Au-MWCNTs) via Cysteaminium Chloride Functionalization, Sci. Rep. 9 (2019) 1–9. https://doi.org/10.1038/s41598-019-42055-7.
27. L. Zhong, J. Zhuang, D.P. Yang, D. Tang, Eggshell membrane-templated synthesis of 3D hierarchical porous Au networks for electrochemical nonenzymatic glucose sensor, Biosens. Bioelectron. 96 (2017) 26–32. https://doi.org/10.1016/j.bios.2017.04.038.
28. Zhao, J. Chu, S.H. Li, W.W. Li, G. Liu, Y.C. Tian, H.Q. Yu, Non-Enzymatic Electrochemical Detection of Glucose with a Gold Nanowire Array Electrode, Electroanalysis. 26 (2014) 656–663. https://doi.org/10.1002/elan.201300565.
29. Wu, L., Lu, Z., & Ye, J., Enzyme-free glucose sensor based on layer-by-layer electrodeposition of multilayer films of multi-walled carbon nanotubes and Cu-based metal framework modified glassy carbon electrode. Biosensors and Bioelectronics, 135(2019), 45-49. https://doi.org/10.1016/j.bios.2019.03.064.
30. Wang, X. Cao, X. Wang, S. Yang, R. Wang, Electrochemical oxidation and determination of glucose in alkaline media based on Au (111)-like nanoparticle array on indium tin oxide electrode, Electrochim. Acta. 138 (2014) 174–186. https://doi.org/10.1016/j.electacta.2014.06.116.
31. Kangkamano, A. Numnuam, W. Limbut, P. Kanatharana, P. Thavarungkul, Chitosan cryogel with embedded gold nanoparticles decorated multiwalled carbon nanotubes modified electrode for highly sensitive flow based non-enzymatic glucose sensor, Sensors Actuators, B Chem. 246 (2017) 854–863. https://doi.org/10.1016/j.snb.2017.02.105.
32. J.S. Ahammad, A. Al Mamun, T. Akter, M.A. Mamun, S. Faraezi, F.Z. Monira, Enzyme-free impedimetric glucose sensor based on gold nanoparticles/polyaniline composite film, J. Solid State Electrochem. 20 (2016) 1933–1939. https://doi.org/10.1007/s10008-016-3199-2.

33. Xu, Y. Song, Y. Ye, C. Gong, Y. Shen, L. Wang, L. Wang, A novel flexible electrochemical glucose sensor based on gold nanoparticles/polyaniline arrays/carbon cloth electrode, Sensors Actuators, B Chem. 252 (2017) 1187–1193. https://doi.org/10.1016/j.snb.2017.07.147.

# Tables

### Table1

Comparison of the Au-SWCNHs/Au electrode with other non-enzymatic glucose electrodes.

| Electrode matrix | Linear range (mM) | Sensitivity (μA $mM^{-1}$ $cm^{-2}$) | Detection limit(mM) | Linear range (mM) | Sensitivity (μA $mM^{-1}$ $cm^{-2}$) | Ref. |
|---|---|---|---|---|---|---|
| AuNPfilm/FTO glass | 0.01-10 | 10.65 | 2 | - | - | 25 |
| AuNPfilm/ITO glass | 0-11 | 23 | 5 | - | - | 30 |
| Au NPs/GONR/CS | 0.005-4.92 | 59.1 | 5 | 4.92-10 | 31.4 | 19 |
| AuNPs-MWCNTs-CS cryogel/AuE | 0.001-1 | 27.7 | 0.5 | - | - | 31 |
| AuNP/PANI/GCE | 0.001-1 | 27.7 | 500 | - | - | 32 |
| AuNP/PANI/CC | 0.01026-10 | 150 | 3.08 | - | - | 33 |
| Au-SWCNHs/Au | 0.5-2 | 275.33 | 0.72 | 4-12 | 352.5 | This work |

AuNp: gold nanoparticle; FTO: fluorine-doped tin oxide; ITO: indium tin oxide; GONR: Graphene Oxide Nanoribbon; CS: Chitosan; AuE: Au electrode; MWCNTs: multi-walled carbon nanotubes; PANI: polyaniline; GCE: glass carbon electrode; CC: carbon cloth; SWCNHs: single-walled carbon nanohorns

### Table 2

The detection of glucose in human serum by the Au-SWCNHs/Au electrode.

| Sample | Original(mM) | Added(mM) | Found(mM) | Recovery(%) |
|---|---|---|---|---|
| Sample 1 | 0 | 1 | 0.97 | 97.00 |
| | 0 | 2 | 1.92 | 96.00 |
| | 0 | 3 | 2.93 | 97.67 |
| Sample 2 | 1 | 1 | 1.87 | 93.50 |
| | 1 | 2 | 2.82 | 94.00 |

# Figures

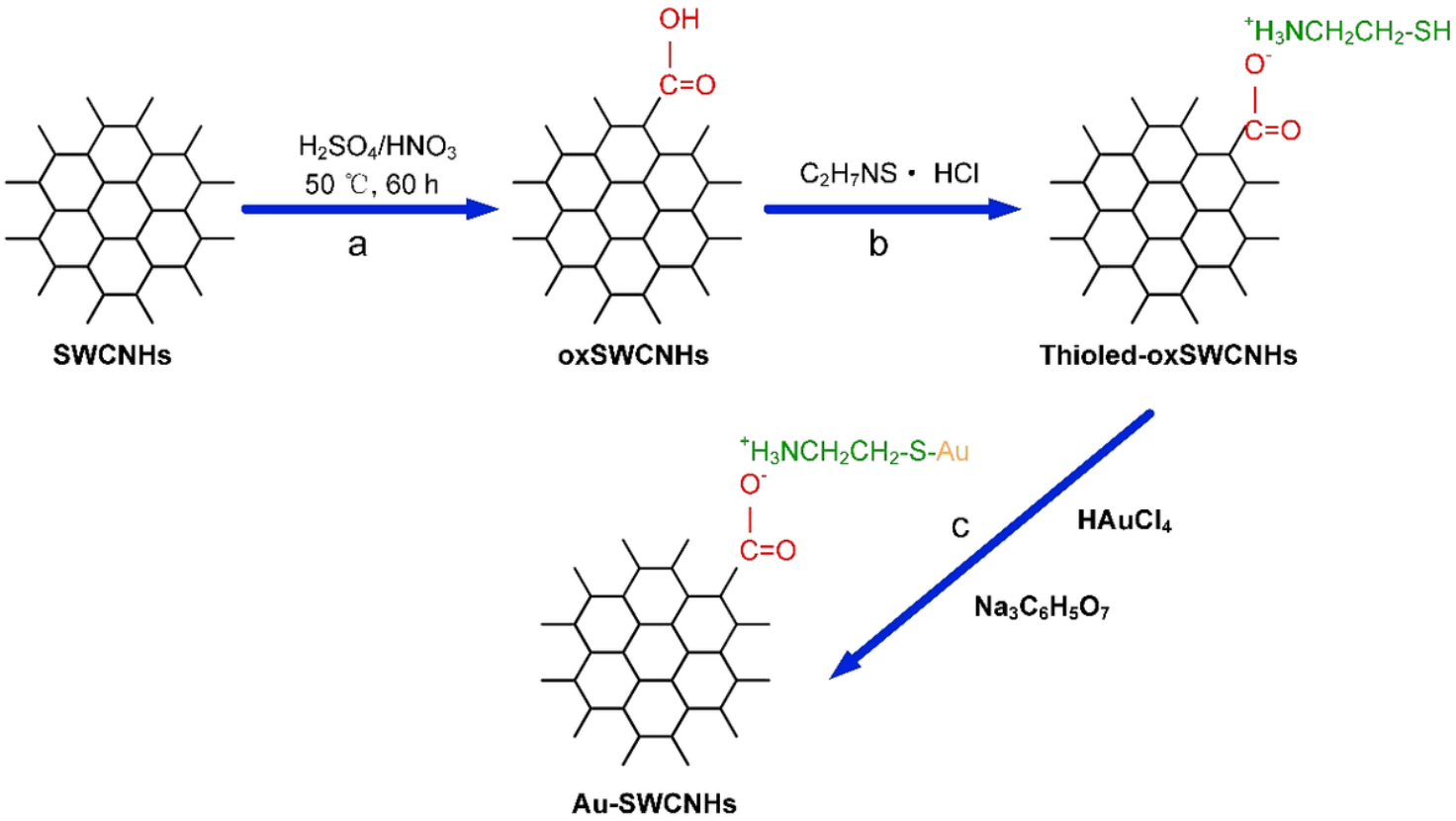


**Figure 1**

Preparation of Au-SWCNHs. a. The oxSWCNHs were prepared via a modified Hummers method. b. The -SH was introduced on the surface of oxSWCNHs. c. The H+ of -SH was replaced by the Au3+ of HAuCl4, and then Au3+ was reduced by Na3+C6H5O7 to AuNp.

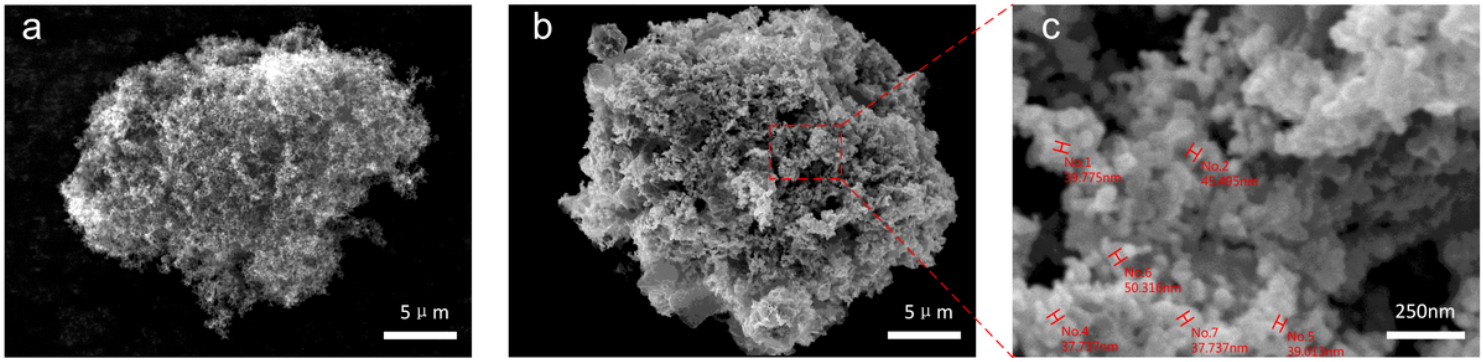


**Figure 2**

SEM images of (a) SWCNHs, (b) Au-SWCNHs composite, and (c) Au-SWCNHs composite (scale bar: 250 nm).

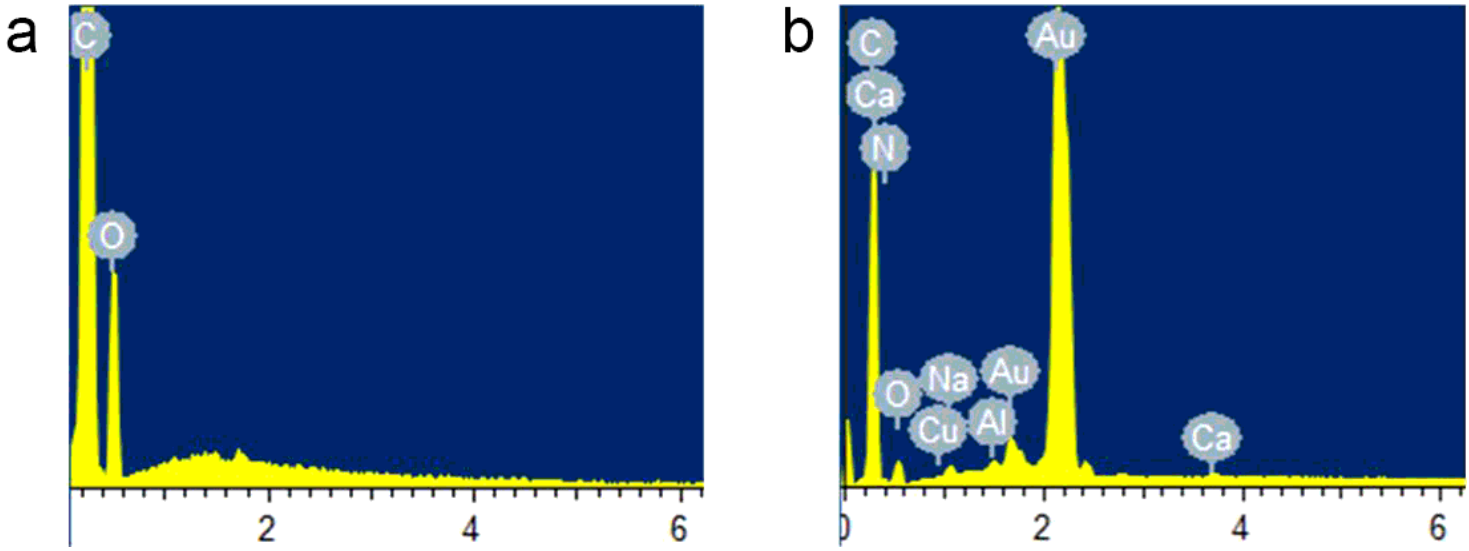


**Figure 3**

Energy spectra of (a) oxSWCNHs and (b) Au-SWCNHs.

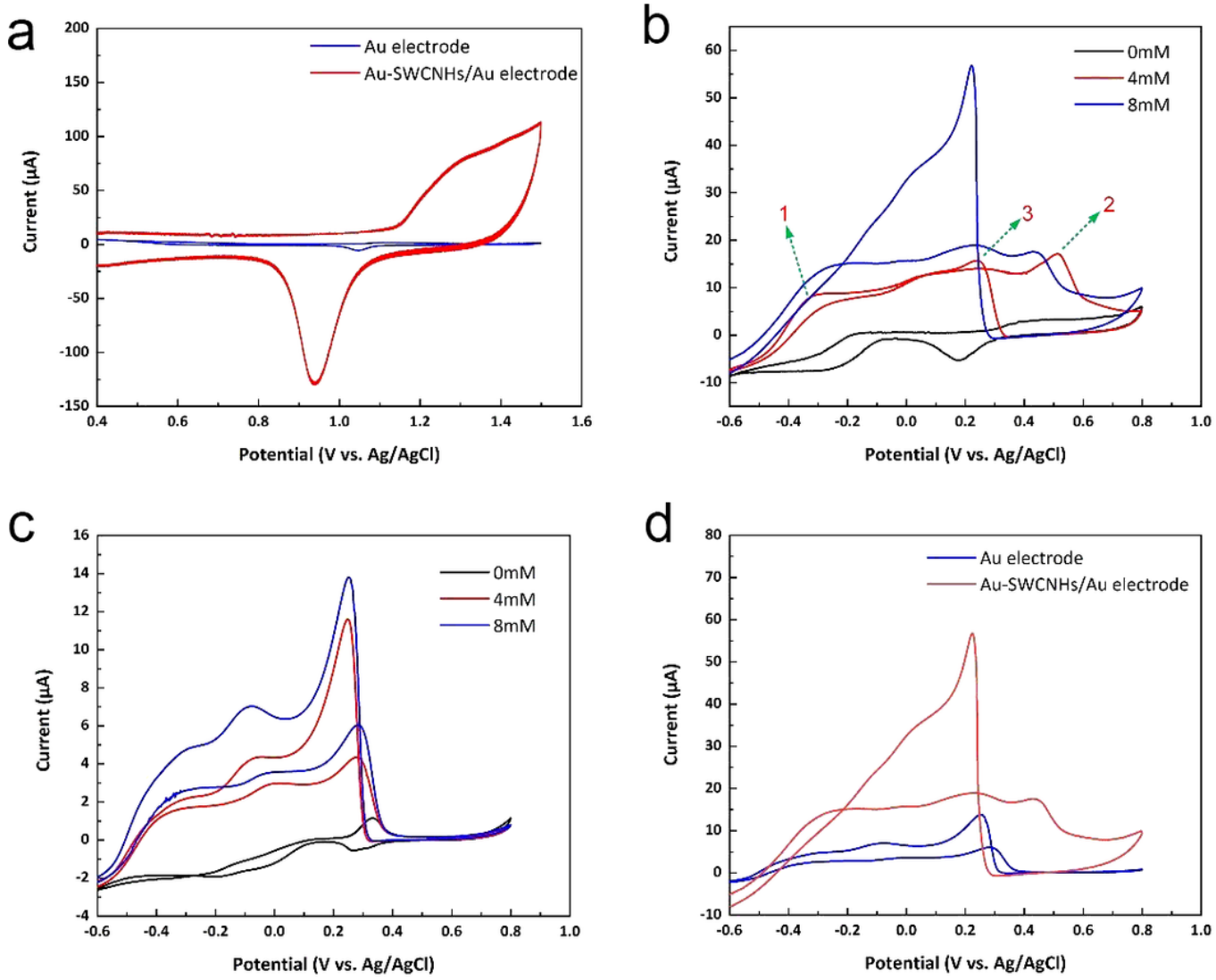


## Figure 4

Cyclic voltammograms of (a) the bare Au electrode (blue) and the Au-SWCNHs/Au electrode (red) in 0.1 M H2SO4 solution, (b) the Au-SWCNHs/Au electrode in 0.1 M NaOH with a glucose concentration of 0, 4, and 8 mM, (c) the bare Au electrode in 0.1 M NaOH with a glucose concentration of 0, 4, and 8 mM, (d) the bare Au electrode (blue) and Au-SWCNHs/Au (red) electrodes in 0.1 M NaOH with a glucose concentration of 8 mM.

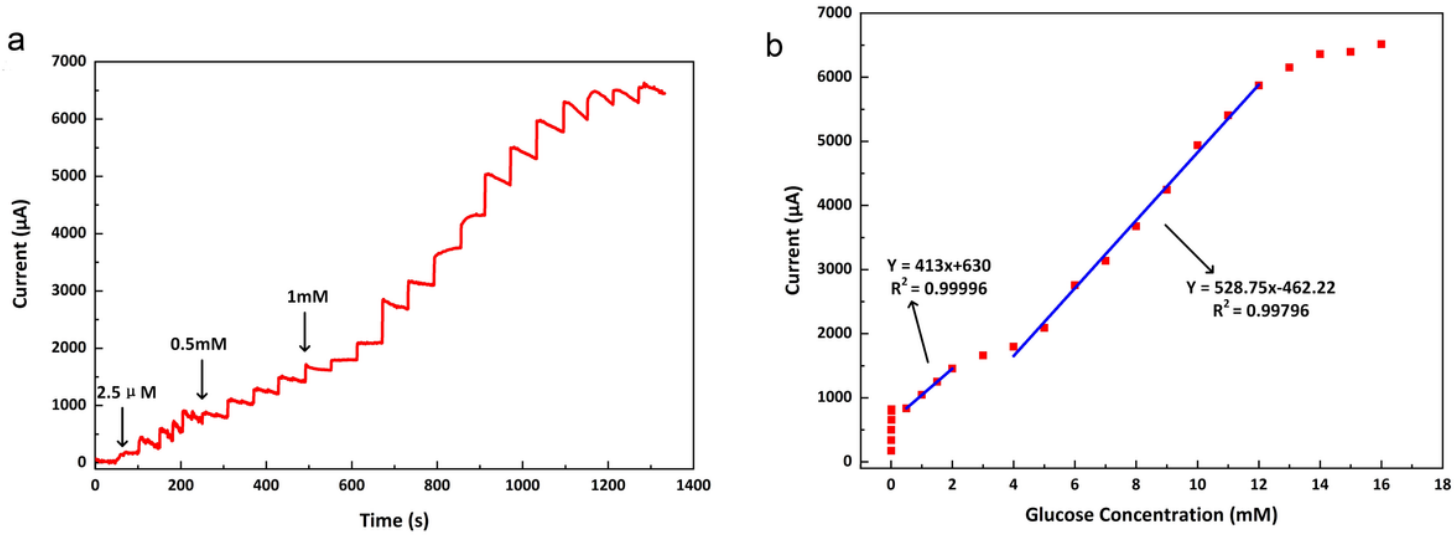


## Figure 5

(a) Amperometric responses of the Au-SWCNHs/Au electrode to various concentrations of glucose. (b) Calibration curve of the current and the corresponding glucose concentration.

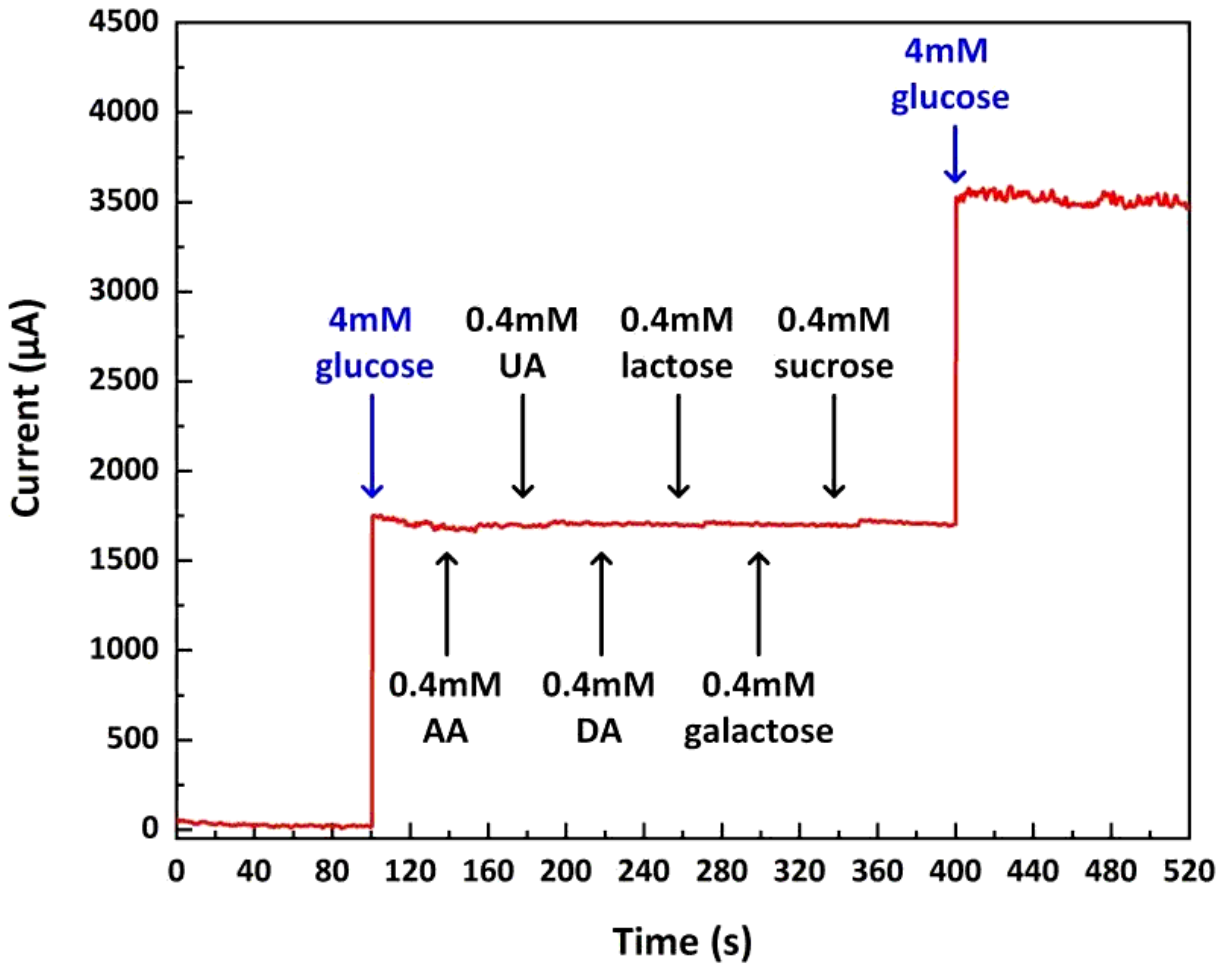


**Figure 6**

Amperometric response of the Au-SWCNHs/Au electrode to successive injections of glucose (4 mM) and ascorbic acid (AA 0.4 mM), uric acid (UA 0.4 mM), dopamine (DA 0.4 mM), lactose (0.4 mM), galactose (0.4 mM), and sucrose (0.4 mM).

## Supplementary Files

This is a list of supplementary files associated with this preprint. Click to download.

- SupportingInformation.docx